Progress In Electromagnetics Research C, Vol. 69, 11–18, 2016

Design of UWB Monopole Antenna for Oil Pipeline Imaging

Richa Chandel[1], Anil K. Gautam[1, *], and Binod K. Kanaujia[2]

Abstract—A novel miniaturized design of UWB monopole antenna is presented and investigated for oil pipeline imaging. In the proposed antenna, an annular-ring shaped radiating patch, slotted ground plane and a feed-line embedded with a semicircular stub are used to enhance the bandwidth. The slotted ground-plane has two extended rectangular strips on its two sides to excite the lower frequency resonance. The proposed antenna design exhibits an enhanced bandwidth of 22 GHz from 3 to 25 GHz (for return loss < 10 dB) which provides a wide usable fractional bandwidth of more than 157% with a compact size of 15 mm$\times$12 mm. Simulated and measured results are discussed to validate the proposed antenna design with enhanced wide bandwidth performance.

1. INTRODUCTION

Ultra wideband (UWB) technology has a wide variety of applications in short-range high data rate communications and radar near-field imaging. For example, microwave holography is used for tissue imaging, radar near-field imaging in crude oil pipeline imaging to study the corrosion, and monitoring the subsurface conditions of different objects. The critical requirement for pipeline inspection using radar imaging is that antenna needs to be operated in crude oil of dielectric constant 2.5, and the size of the antenna should be as small as possible. As the image resolution is directly proportional to the bandwidth of the pulse, all the imaging applications require wide bandwidth. Microstrip antenna with different shapes such as octagonal-shaped, arc-shaped, M-shaped, annular slot, hexagonal shaped, beak-shaped, M-shaped, triangular [1–8] geometries have been proposed for UWB application. In [9], a C-shaped radiators with an inverted L-shaped coupled strip extending from the ground plane is used for bandwidth enhancement, whereas coupling effect between the structures is used to improve the impedance matching. A planar crossed monopole antenna [10] and a rectangular patch with U-shaped open-slot structure [11] have been reported for UWB application. Folded ramp-shape feeding techniques is used for enhanced bandwidth, and shorting pins are used to miniaturize the size of the patches [12]. A novel compact microstrip-fed UWB step-slot antenna with a rotated patch for enhanced impedance bandwidth is demonstrated in [13]. All the antennas discussed above are larger in size and offers a relatively lower impedance bandwidth than the proposed antenna design. Further reduction of the antenna size would face a challenge as the sizes of these antennas are determined by the longest electrical length of the surface currents at the lowest frequency.

In the present study, a miniaturized design is proposed and investigated for wideband applications using a microstrip-line fed annular-ring monopole radiator for oil pipeline imaging. In the proposed design, an annular-ring shaped radiating patch and defected ground plane are used with an embedded semicircular stub in the feed-line to obtain enhanced bandwidth. The slotted ground-plane has two extended rectangular strips on both sides, which excites an additional resonance at lower frequency. The antenna can be easily fit into a pipeline without obstructing the flow of the liquids. The antenna is also able to provide seamless operation in crude oil.

Received 9 June 2016, Accepted 26 August 2016, Scheduled 26 October 2016

* Corresponding author: Anil K. Gautam (drakgautam@ieee.org).

[1] Department of Electronics & Communication Engineering, G. B. Pant Engineering college, Pauri Garhwal, Uttarakhand-246194, India. [2] Department of Electronics & Communication Engineering, Ambedkar Institute of Advanced Communication Technologies & Research, Geeta Colony, Delhi-110031, India.

2. ANTENNA DESIGN

Figure 1 shows a schematic configuration of the proposed geometry which is fed by a 2.4 mm wide microstrip line. The antenna is fabricated on an epoxy FR4 dielectric substrate (loss tangent, $\tan\delta = 0.02$, relative permittivity, $\epsilon_r = 4.4$) with very small dimensions of $15\times12\times1.6\,\text{mm}^3$. The radiator consists of two annular-rings that are printed one over the other along with a rectangular strip of width W_f and length L_{p2}. The feed is modified by attaching a semicircular stub of r_5 to provide $50\,\Omega$ feed and to improve impedance matching. The slotted ground plane of the proposed antenna is printed on the other side of the dielectric substrate to improve impedance matching at the lower middle band. Further, two rectangular strips of lengths L_{g1} and L_{g2} of width W_{g1} are connected at the edges of ground plane to excite lower frequency band. It is clearly observed from Table 1 that the proposed antenna has the smallest size with enhanced bandwidth from the above reported designs.

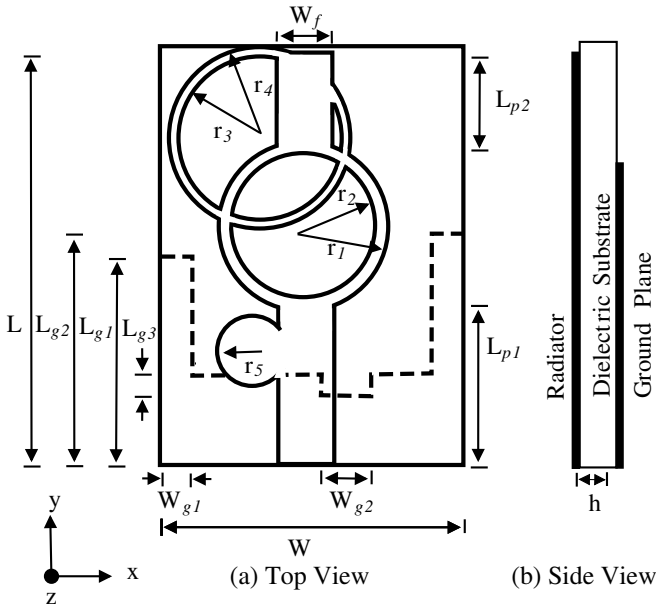

Figure 1. Schematic configuration of the proposed prototype.

Table 1. Performance comparison of the proposed antenna with other reported antennas.

Reference #	Size mm×mm	Operating Bands (GHz)
[1]	70×60	2.5–18
[2]	30×30	3.02–13.27
[3]	36×36	2.38–12.40
[4]	80×80	3–12
[5]	25×23	2.71–12.61
[6]	24×24	0.24–24.5
[7]	23×41	2.3–20
[8]	30×30	3–12
[9]	25×40	3.1–5.15
[10]	20×20	3.1–10.6
[11]	24.5×24.5	2.95–12.1
Proposed	**15×12**	**3.0–25**

Table 2. Design parameters of the proposed antenna shown in Fig. 1.

Parameters	L_{p1}	L_{p2}	W_f	r_1	r_2	r_3	r_4
Unit(mm)	4.53	4.28	2.4	3.2	2.8	3.2	3.5
Parameters	W_{g1}	W_{g2}	L_{g3}	L_{g1}	L_{g2}	r_5	W
Unit (mm)	1.5	1.5	1	7.0	7.5	1.3	12

The antenna design was implemented in three steps, as demonstrated in Fig. 2. Step one involves construction of the feed-line with a simple annular shaped patch; the second step is modified by attaching a semicircular conductor to the feed line; and the final step involves creating another annular-ring on upper side of the annular patch. The return loss responses of the antenna in all three steps are depicted in Fig. 2. Thus the proposed antenna provides a ultra wideband with a usable fractional bandwidth of more than 157% (3–25 GHz). The parameters of the proposed geometry are optimized to achieve a miniaturized design, and optimized dimensions are listed in Table 2.

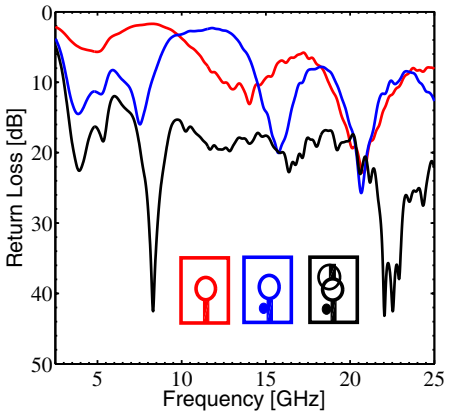

Figure 2. Simulated return loss against frequency for three steps that are used for designing the antenna.

The various simulated current densities are plotted in Fig. 3. to understand the enhanced wideband behaviour of the antenna. Fig. 3(a) depicts that the surface current is mainly distributed over the entire ground plane and lower annular ring of the patch. It clearly indicates that the lower band is excited due to both the rectangular strips attached to the ground plane and a lower annular ring. The surface currents are mainly distributed over the ground plane and central parts of the radiator for the frequency around 6 GHz [see Fig. 3(b)]. For middle frequencies around 16 GHz, the current is concentrated around annular rings of the patch and feed-line as shown in Fig. 3(c). Finally, Fig. 3(d) shows that the current is distributed over entire patch and ground plane.

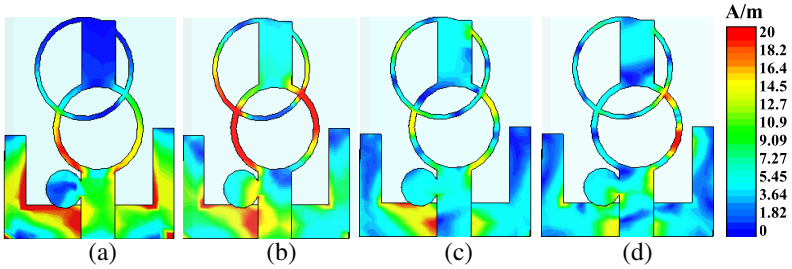

Figure 3. Simulated surface current distribution of the proposed antenna at (a) 3.9 GHz, (b) 6 GHz, (c) 16 GHz, and (d) 22 GHz frequencies.

2.1. Parametric Study

Simulated return loss curves for various parameters of the antenna are discussed in order to show the effectiveness of the designed antenna. Fig. 4(a) depicts the variation of the outer radius (r_1) of annular ring with frequency. It is observed that for the outer radius $r_1 = 3.2$ mm, the antenna shows enhanced impedance bandwidth from 3–25 GHz. Therefore, r_1 is used to enhance impedance bandwidth and improve impedance mismatch that mainly occurs at middle (7–13 GHz) and higher frequency bands. Fig. 4(b) depicts the return loss curve of the parameter (r_5), i.e., radius of the semicircular stub attached to the feed-line with frequency. As the value of r_5 increases from 0.9 mm to 1.3 mm, impedance matching greatly improves. It is found that return loss of the antenna remains below 10 dB for $r_5 = 1.3$ mm. Further increment in the value of r_5 degrades the performance of the antenna. Therefore, at $r_5 = 1.3$ mm the antenna shows enhanced impedance bandwidth from 3–25 GHz.

In the proposed antenna design, the ground plane parameters significantly controls the impedance bandwidth of the antenna. In order to get the best performance, various simulations were carried out. The rectangular strips extended on both sides of ground plane excite the first resonance in the proposed antenna. Fig. 5(a) shows the return loss curves of the proposed antenna for various ground strip lengths (L_{g1}) with frequency. It is observed that for length $L_{g1} = 7$ mm, the antenna shows enhanced impedance bandwidth from 3–25 GHz. Therefore, L_{g1} is used to improve impedance matching at the lower and

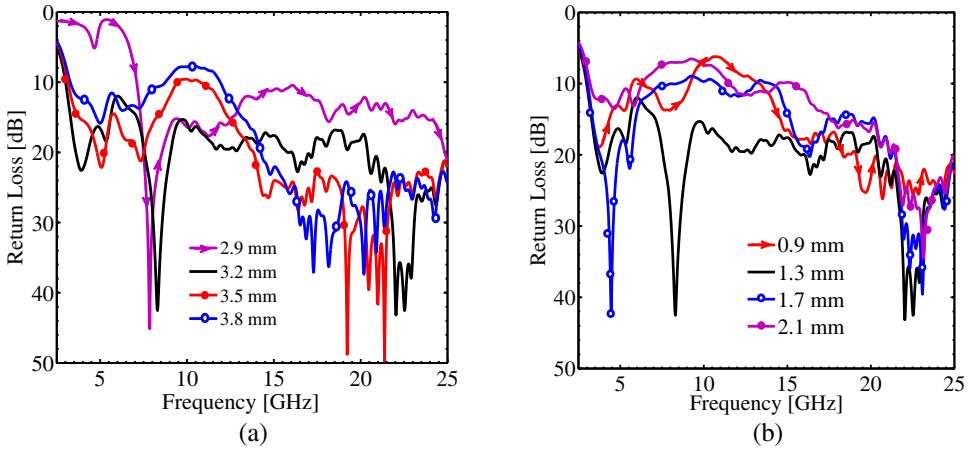

Figure 4. Simulated return loss against frequency of the proposed antenna with radius, (a) r_1 and (b) r_5.

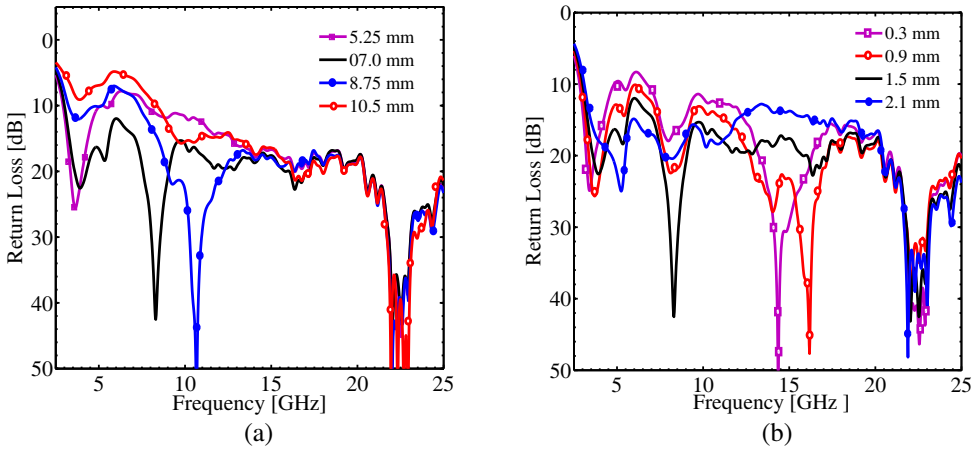

Figure 5. Simulated return loss against frequency of the proposed antenna with length and width (a) L_{g1} and (b) W_{g1}.

middle frequency bands. The width W_{g1} of the rectangular strip also affects the performance of the antenna. Fig. 5(b) shows the simulated return loss curve of the proposed antenna for various ground strip widths W_{g1} with frequency. As the value of W_{g1} increases from 0.3 mm to 2.1 mm, the impedance matching mainly at lower frequency band improves. Therefore, at $W_{g1} = 1.5$ mm the antenna shows enhanced impedance bandwidth from 3–25 GHz.

3. TIME DOMAIN ANALYSIS

The pulse handling capability along with fidelity factor calculation of the proposed antenna is measured by time-domain analysis using CST MWS. These studies are carried out by placing two antennas (transmitter and receiver) in the far-field region (face-to-face and side-by-side). The transmitter is excited by a Gaussian signal that complies with the FCC indoor and outdoor power spectrum mask. Fig. 6 shows the input and received signals in the far-field region (side-by-side and face-to-face).

The low-distortion time domain performance of the miniaturized antenna is also confirmed by calculating the fidelity factor. Fidelity factor is used to measure the degree of similarity or correlation between the transmitted and received pulses. Fidelity factor can be calculated using the following

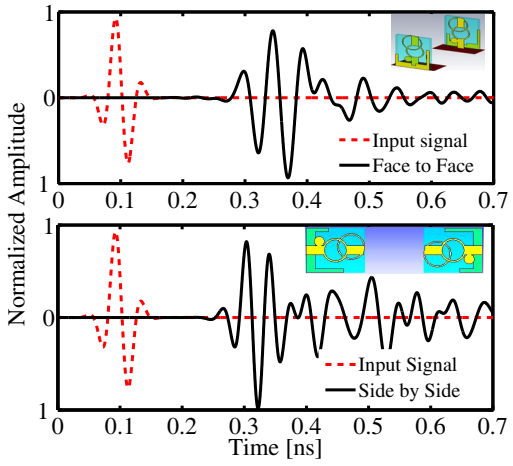

Figure 6. Input and received pulse in different orientations of proposed antenna.

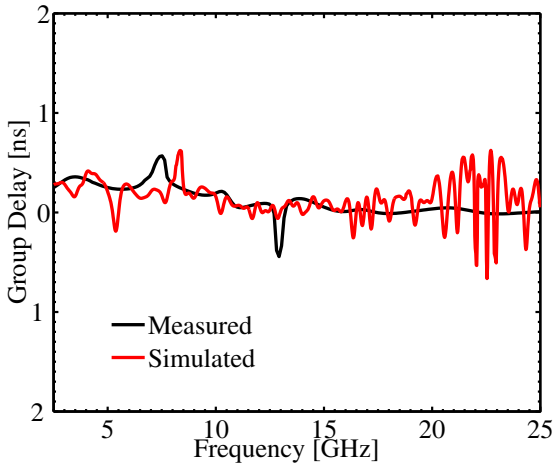

Figure 7. Group Delay of the proposed antenna.

equation

$$F = \max \left| \frac{\int_{-\infty}^{\infty} s_t(t) s_r(t+\tau) dt}{\sqrt{\left(\int_{-\infty}^{\infty} s_t(t)^2 dt\right)\left(\int_{-\infty}^{\infty} s_r(t)^2 dt\right)}} \right| \tag{1}$$

where $s_t(t)$ and $s_r(t)$ are input and received signals. The fidelity factors in the case of face-to-face and side-by-side are obtained as 73% and 61%, respectively. The group delay is another parameter in time domain analysis, which shows the distortion of the transmitted pulses in the wideband communication. Therefore, the group delay shall be almost constant in the entire operating band for a good pulse transmission. It is seen from Fig. 7 that the group delay of the proposed antenna remains constant as it shows a variation of 1 ns only. The group delay characteristics discussed above demonstrate that the proposed antennas exhibit phase linearity at desired operating frequencies. It is found, from the aforesaid parametric studies in the time domain, that the antenna has a good pulse handling capability in the entire operating frequency band.

4. RESULT AND DISCUSSION

After optimization, the proposed antenna was fabricated with the MITS-Eleven Lab PCB machine. Then to validate the simulated results, the antenna return loss is measured by submerging the antenna in diesel using the Agilent N5230A vector network analyzer. Diesel has the same dielectric constant as crude oil [14]. Fig. 8 shows the variations of the return loss with frequency for the proposed enhanced bandwidth antenna. It is found that the antenna shows an enhanced wide bandwidth for return loss < 10 dB of 22 GHz (from 3–25 GHz). The measured result shows good agreement with simulated one. Some deviation from the simulated result may be due to fabrication tolerance or measurement as it is carried out in the scattering environment.

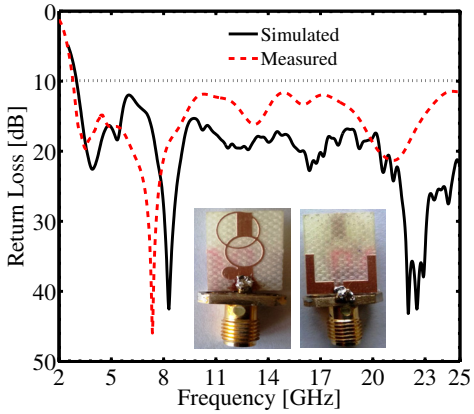

Figure 8. Return loss variation with frequency for proposed antenna.

The variations of the gain and the radiation efficiency with the frequency of the proposed antenna are shown in Fig. 9. It is evident that the antenna shows a good radiation efficiency for the entire band of operation within 75% to 90%. It is also observed from Fig. 9 that the gain of the proposed antenna varies from 2.8 dB to 5.8 dB. Thus, the gain of the proposed antenna remains stable, and its low value is due to very compact size of the antenna.

Figure 10 shows the measured radiation patterns in the xy-, yz- and xz-planes at various sampling frequencies (3.9, 6.5, 16.5 and 22 GHz). It is seen that the radiation pattern is like a monopole antenna pattern at the lower frequency side (3 GHz). At higher frequencies, the radiation is due to the higher-order modes which are responsible for splitting of the radiation lobe.

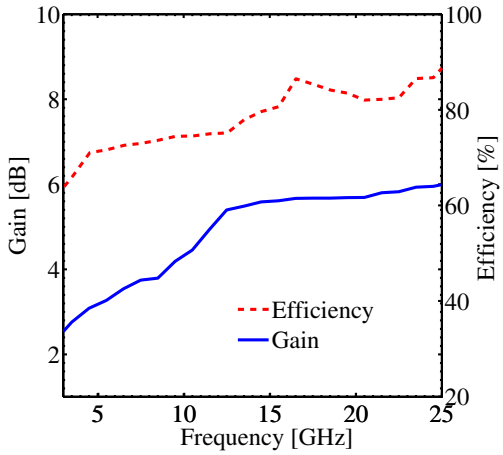

Figure 9. Gain and Radiation efficiency of the proposed UWB antenna.

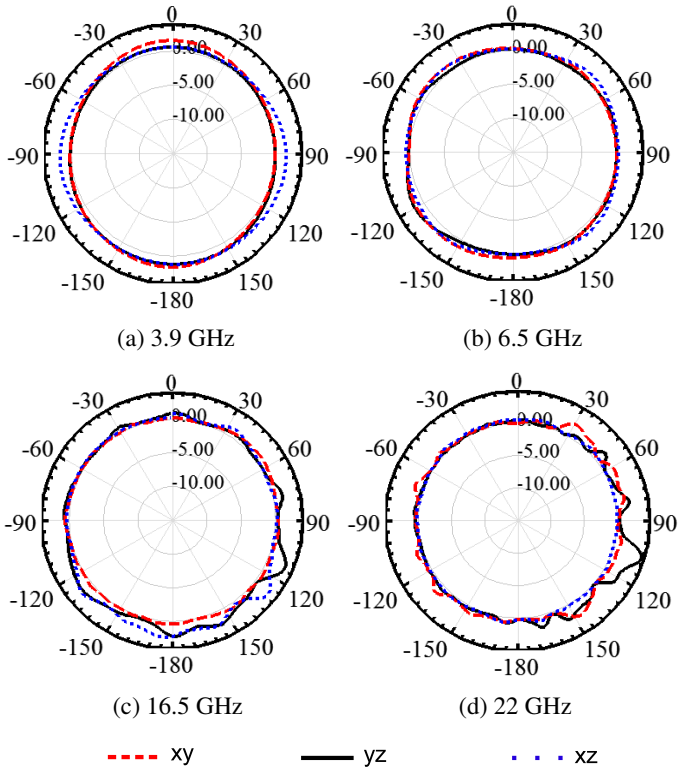

Figure 10. Radiation patterns of proposed antenna at various frequencies.

5. CONCLUSION

We have proposed a novel miniaturized design of a UWB monopole antenna for enhanced wide bandwidth performance. The proposed antenna offers an impedance bandwidth of 22 GHz (from 3–25 GHz) with a good impedance matching and stable radiation pattern. As the size of the antenna is very small, it is a potential candidate for pipeline inspection using radar imaging.

REFERENCES

1. Dikmen, C. M., S. Cimen, and G. Cakr, "Planar octagonal-shaped UWB antenna with reduced radar cross section," *IEEE Transactions on Antennas and Propagation*, Vol. 62, No. 6, 2946–2953, 2014.
2. Lu, J. H. and C. HsuanYeh, "Planar broadband arc-shaped monopole antenna for UWB system," *IEEE Transactions on Antennas and Propagation*, Vol. 60, No. 7, 3091–3095, 2012.
3. Shrivastava, M. K., A. K. Gautam, and B. K. Kanaujia, "An M-shaped monopole-like slot UWB antenna," *Microwave and Optical Technology Letters*, Vol. 56, No. 1, 127–131, 2014.
4. Gallo, M., E. A. Daviu, M. F. Bataller, M. Bozzetti, J. M. M. G. Pardo, and L. J. Llacer, "A broadband pattern diversity annular slot antenna," *IEEE Transactions on Antennas and Propagation*, Vol. 60, No. 3, 1596–1598, 2011.
5. Gautam, A. K., R. Chandel, and B. K. Kanaujia, "A CPW-fed hexagonal-shape monopole-like UWB antenna," *Microwave and Optical Technology Letters*, Vol. 55, No. 11, 2624–2628, 2013.
6. Chandel, R., A. K. Gautam, and B. K. Kanaujia, "Microstrip-Line fed beak-shaped monopole-like slot UWB antenna with enhanced band width," *Microwave and Optical Technology Letters*, Vol. 56, No. 11, 2624–2628, 2014.
7. Deng, C., Y. J. Xie, and P. Li, "CPW-fed planar printed monopole antenna with impedance bandwidth enhanced," *IEEE Antenna and Wireless Propagation Letters*, Vol. 8, 1394–1397, 2009.
8. Lin, C. C. and H. R. C. Lin, "A 3–12 GHz UWB planar triangular monopole antenna with ridged ground-plane," *Progress In Electromagnetics Research*, Vol. 83, 307–321, 2008.
9. Kim, G. H. and T. Y. Yun, "Compact ultrawideband monopole antenna with an inverted-L-shaped coupled strip," *IEEE Antenna and Wireless Propagation Letters*, Vol. 12, 1291–1294, 2013.
10. Ghosh, S., "Design of planar crossed monopole antenna for ultrawideband communication," *IEEE Antenna and Wireless Propagation Letters*, Vol. 10, 548–551, 2011.
11. Liu, W., Y. Yin, W. Xu, and S. Zuo, "Compact open-slot antenna with bandwidth enhancement," *IEEE Antenna and Wireless Propagation Letters*, Vol. 10, 850–853, 2011.
12. Malekpoor, H. and J. Shahrokh, "Enhanced bandwidth of shorted patch antennas using folded-patch techniques," *IEEE Antenna and Wireless Propagation Letters*, Vol. 12, 198–201, 2013.
13. Song, K., Y. Z. Yin, B. Chen, S. T. Fan, and F. Gao, "Bandwidth enhancement design of compact UWB step-slot antenna with rotated patch," *Progress In Electromagnetics Research Letters* Vol. 22, 39–45, 2011.
14. Kumar, T., A. K. Gautam, B. K. Kanaujia, and K. Rambabu, "Design of miniaturised UWB antenna for oil pipeline imaging," *Electronics Letters*, Vol. 51, No. 21, 1626–1628, 2015.